

# Plasmonic waveguide as an efficient transducer for high-density data storage

D. O'Connor,<sup>1</sup> M. McCurry,<sup>2</sup> B. Lafferty,<sup>2</sup> and A. V. Zayats<sup>1,a)</sup>

<sup>1</sup>Centre for Nanostructured Media, The Queen's University of Belfast, Belfast BT7 1NN, United Kingdom

<sup>2</sup>Seagate Technology, 1 Disc Drive, Derry BT48 0BF, United Kingdom

(Received 17 July 2009; accepted 9 October 2009; published online 30 October 2009)

A design of high optical throughput nanoscale light sources has been proposed based on plasmonic wedge waveguides. It provides localization of the 1500 nm wavelength light at the output of less than  $30 \times 30 \text{ nm}^2$  area at about 80% coupling efficiency from a dielectric loaded surface plasmon polariton waveguide and nearly 90% efficient power deposition in the absorbing media placed at the output for an experimentally viable 10 nm apex radius of the wedge. Such nanoscale light sources can be useful for high-density data storage, scanning near-field optical microscopy, and sensing.  
© 2009 American Institute of Physics. [doi:10.1063/1.3257701]

As the areal density of digital data storage increases toward the Tb/in<sup>2</sup> regime, the dimensions of individual bits shrink down to below 500 nm<sup>2</sup> size. Manipulation of data on such dimensions in optical, magneto-optical, and indeed magnetic media relying on heat-assisted magnetic recording (HAMR) requires development of viable optical means of efficient confinement and delivery of high power light to nanometer-sized areas.<sup>1,2</sup>

For example, a practical HAMR system based on laser heating of individual bits during magnetic recording to overcome high coercivity of the a magnetic material used to exceed superparamagnetic limit should provide high confinement down to  $\sim 25 \times 25 \text{ nm}^2$  (for an areal density of 1 Tb/in<sup>2</sup>) and a power flow of about 1 mW needed in order to deliver a sufficient amount of energy to heat the target region during the transit time of the write head.<sup>2</sup> Moreover, the availability of wavelengths, powers, and sizes of integratable light sources suitable for this purpose [e.g., vertical-cavity surface-emitting laser (VCSELs) or edge-emitting lasers] implies that an intermediate light guiding system must also be considered.

Strong light confinement can be efficiently achieved with various types of nanoscale apertures and nanoantennas but at the expense of power throughput even in the most sophisticated plasmonic structures such as bow-tie and bullseye type geometries.<sup>3,4</sup> Recently, a "superlensing" effect with

a planar plasmonic lens and plasmonic nanoparticle concentrator has been proposed for the use in HAMR.<sup>5,6</sup> A metal-insulator-metal taper has also been modeled and optimized for high power throughput.<sup>7</sup> The coupling efficiency of about 8% into  $74 \times 80 \text{ nm}$  spot in a recording medium at 830 nm has been achieved using two coupled disks.<sup>6</sup> The outcoupling into a perfectly matched layer with mode size  $21 \times 24 \text{ nm}$  at 1550 nm with 62% efficiency numerically predicted using tapered metal-insulator-metal waveguide.<sup>7</sup>

In this letter we examine a complete plasmonic route toward a high brightness nanoscale light source based on plasmonic wedge waveguides. With this approach, a low loss guiding system and nanoscale confinement can be naturally integrated in a single device. The plasmonic waveguide can also be easily coupled to a VCSEL light source. Other potential applications of the proposed approach can be in scanning near-field optical microscopy and sensing.

A surface plasmon polariton (SPP) is a coupled excitation of charge oscillations at the surface of a metal and a momentum matched electromagnetic field oscillation that is bound to the interface and propagates as wave. SPPs naturally provide field confinement in the direction normal to the surface, due to their wave vector in the direction of propagation always being greater than the equivalent free space wave vector. The reduced SPP wavelength gives some benefits

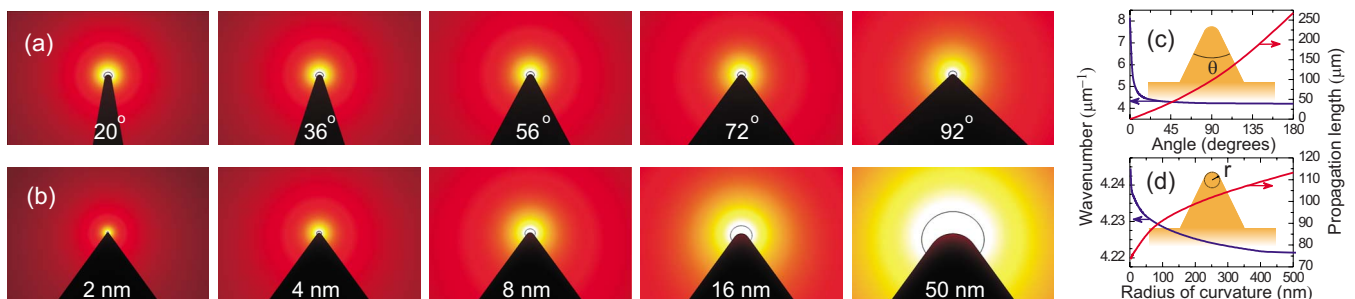


FIG. 1. (Color online) [(a) and (b)] Electromagnetic intensity distributions with the marked  $1/e$  distance of the energy localization calculated for (a) various opening angles for  $r=10 \text{ nm}$  and (b) various apex curvatures  $r$  for  $\theta=72^\circ$ . [(c) and (d)] Wave number and propagation length dependence on the given structural parameter at a fixed 1500 nm free space wavelength. The inset in [(c) and (d)] illustrates the geometry of the system. The rail height is 2000 nm. The rail is surrounded by air.

<sup>a)</sup>Electronic mail: a.zayats@qub.ac.uk.

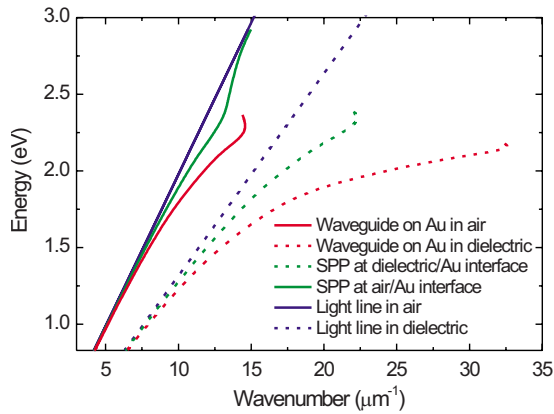


FIG. 2. (Color online) Dispersion curves for a rail waveguide with  $72^\circ$  opening angle, 2 nm apex radius and 2000 nm height in air  $n=1$  (solid lines) and dielectric  $n=1.5$  (dashed lines). The light lines and SPP dispersions on a smooth metal interface are shown for comparison in both cases.

when considering applications in waveguide minituriation and two-dimensional focusing elements.<sup>8,9</sup>

The control over the SPP wavelength provided by the geometrical parameters of metallic nanostructures offers a possibility to design truly deep-subwavelength, nanoscale waveguides with size not limited by the light wavelength. Thus, nanoscale plasmonic waveguides can be used for achieving nanoscopic light sources needed in various applications. An increase in the plasmonic field confinement however inevitably leads to the increase in the propagation loss of plasmonic waveguides due to Ohmic losses in metals.

Recently, another type of plasmonic waveguides has been proposed based on V-shaped ridges that can provide strong confinement and sufficiently low propagation loss.<sup>10–12</sup> In this geometry, a wedgelike fold introduced in the planar surface of metal [inset in Fig. 1(c)] changes the effective refractive index of the supported SPPs and thus results in the field confinement near the apex of the fold, where the SPP wave vector is larger due to the reduced restoring forces on the charge oscillations in metal.

Numerical simulations using finite element method confirm that there is a confined propagating mode centered at the apex of this rail-like geometry (Fig. 1). The field distribution, mode wave number and propagation length of several of these waveguides were calculated at a fixed wavelength to show the dependence on apex radius of curvature, the interior angle of the rail, the height of the rail as well as the adjacent dielectric medium's refractive index. The analysis

shows that radius of curvature and not only opening angle is a critical parameter for confinement and will allow for the design of robust devices. In the following, the opening angle has been chosen to be  $72^\circ$ , which corresponds to that which is easily achievable with directionally etched silicon templates restricted by silicon crystalline lattice. Apex curvatures as small as 2 nm have been experimentally demonstrated.<sup>13</sup>

The SPP dispersion on the wedge for some representative parameters of the waveguides is shown in Fig. 2. The wedge SPP mode exists in a higher momentum space than the equivalent smooth film SPP at all frequencies. The introduction of the dielectric around the fold further increases SPP wave vector. The use of a dielectric stripe may have further advantages, beyond decreasing the wavelength and increasing the confinement, for coupling of light to these SPP modes e.g., via dielectric-loaded SPP waveguides (DLSPPWs).<sup>9</sup>

As the next step, various coupling schemes from a smooth-film SPP to optimized rail waveguide geometries were simulated. These include those with adiabatic variation of the structural parameters of the rail for a reflection-free focusing of incoming SPPs by the wedge. An example of a practical coupling scheme is shown in Fig. 3 for the coupling from the single-mode dielectric-loaded to wedge-shaped SPP waveguide embedded in the same dielectric. Here, the height of the wedge is varied from zero to the optimal height in an adiabatic manner [elevation angle  $1.43^\circ$  corresponding to adiabatic parameter<sup>14</sup>  $d(1/n_{SPP})/dz \cdot \lambda \sim 0.008$ ], keeping the opening angle and curvature radius the same. When the SPP in the DLSPPW propagates toward the rising fold, the energy is pulled toward the apex leading to the significant field confinement. The coupling efficiency in this scheme, including associated propagation losses was found to be about 79%, i.e., 79% of the energy of the SPP guided in DLSPPW [Fig. 3(a)] is focused at the output situated  $4 \mu\text{m}$  from the input with the field profile ( $11 \times 5 \text{ nm}^2$ ) shown in Figs. 3(b) and 3(e). The loss is mainly due to the Ohmic losses in metal, only about 4% of the energy is reflected for this adiabatic parameter of the rising wedge.

The out-coupling into a target recording medium was simulated in order to show the operating characteristics and total efficiency of this type of nanoscale light source. For this purpose, two-dimensional eigenmode is launched from the source boundary on the left of Fig. 4 at a power of 1 W (arbitrary value chosen to provide simple scaling). As seen

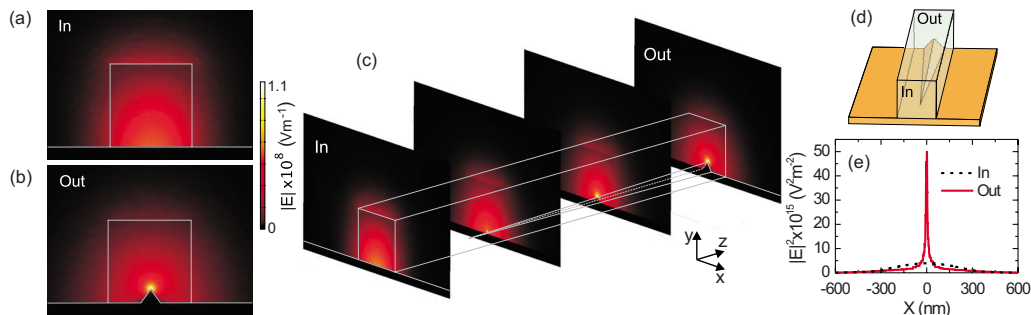


FIG. 3. (Color online) Electromagnetic intensity distribution at the input (a) and output (b) of the rail waveguide schematically shown in (d). (c) Four cross-sections showing the mode variation with the waveguide height. (e) Cross-sections of the intensity distributions at in- and out-coupling interface. A  $72^\circ$  opening angle wedge with 10 nm curvature radius is grown to the height of 100 nm over  $4 \mu\text{m}$  length. The rail is embedded in dielectric strip ( $600 \times 600 \text{ nm}^2$ ) with  $n=1.5$ , corresponding to a single mode SPP guiding at the considered light wavelength of 1500 nm.

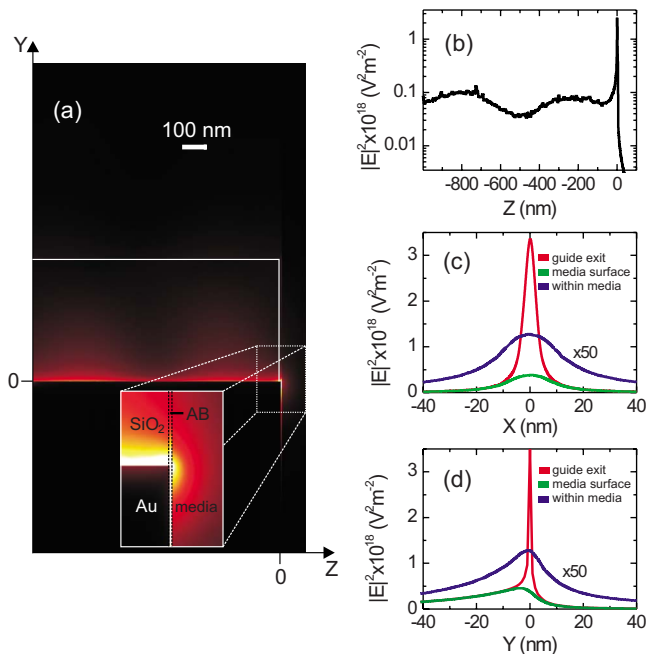


FIG. 4. (Color online) (a) Side view cross-section of the electromagnetic intensity distribution of the SPP guided mode propagating toward the end of the rail-waveguide placed in the vicinity of the recording medium (simulated with  $n_{eff}=2-i$ ). The rail height is 100 nm; the other parameters are the same as in Fig. 3. The thickness of air bearing is 5 nm. The inset shows the zoom in the area where the energy is deposited. [(b), (c), and (d)] The cross-sections along the guide axis, [(b), and (d)], at the exit from the waveguide, at the recording medium surface, and at the distance of 1 nm within the recording medium.

from the side view cross-section, the electric field distribution of the guided mode propagating toward the end of the rail ( $z=0$  nm) placed in the vicinity of the recording medium exhibits periodic modulation due to the interference of the incident and reflected SPP waves. From the depth of this modulation the intensity reflection coefficient was estimated to be less than 4%. When the guided mode reaches the end of the wedge guide, the scattering leads to the excitation of the SPP mode in the air-bearing (AB) layer (thickness 5 nm) as well as scattering light above the waveguide (Fig. 4 and the inset). The numerical measurements shows that only about 6% of the power is scattered at the output, 5% and 4% account for the Ohmic loss and backward reflection, respectively, while 85% propagates toward the recording medium and is absorbed in it. (The difference between the power flow

toward the medium at the exit of the guide and through the medium surface is of the order of 0.2% and is within numerical noise of the calculations). The cross-section in Figs. 4(c) and 4(d) shows the profile of the absorbed energy which is  $30 \times 30$  nm<sup>2</sup> in area compared to  $11 \times 5$  nm<sup>2</sup> of the profile of the energy distribution at the exit of the waveguide.

In conclusion, the scheme for electromagnetic energy confinement, delivery and focusing in less than  $\lambda/100$  mode size with a total conversion efficiency of nearly 80% is demonstrated using adiabatic mode transformation of a SPP on a wedge guide embedded in a single mode DLSPW. The guided mode can be out-coupled at 90% efficiency into a target medium placed within the near-field at nanoscale dimensions [ $30 \times 30$  nm<sup>2</sup> full width at half maximum (FWHM) from a 10 nm apex radius rail and potentially even smaller FWHM from smaller apex wedges]. The overall transmittance of the proposed system is much higher than one achievable with nanoscale apertures and nanoparticles (less than 10%).<sup>2,6</sup> This transmittance is chiefly limited by Ohmic losses in the metal.

This work has been supported in part by Seagate Technology and EPSRC (U.K.). D.O.C. and A.Z. acknowledge fruitful discussions with Alexei Krasavin.

- <sup>1</sup>A. S. van de Nes, J. J. M. Braat, and S. F. Pereira, *Rep. Prog. Phys.* **69**, 2323 (2006).
- <sup>2</sup>T. W. McDaniel, *J. Phys.: Condens. Matter* **17**, R315 (2005).
- <sup>3</sup>W. A. Challener, E. Gage, A. Itagi, and C. Peng, *Jpn. J. Appl. Phys., Part 1* **45**, 6632 (2006).
- <sup>4</sup>H. J. Lezec, A. Degiron, E. Devaux, R. A. Linke, L. Martin-Moreno, F. J. Garcia-Vidal, and T. W. Ebbesen, *Science* **297**, 820 (2002).
- <sup>5</sup>Y. Wang, W. Srituravanich, C. Sun, and X. Zhang, *Nano Lett.* **8**, 3041 (2008).
- <sup>6</sup>W. A. Challener, C. Peng, A. V. Itagi, D. Karns, W. Peng, Y. Peng, X. Yang, X. Zhu, N. J. Gokemeijer, Y.-T. Hsia, G. Ju, R. E. Rottmayer, M. A. Seigler, and E. C. Gage, *Nature Photon.* **3**, 220 (2009).
- <sup>7</sup>R. Yang, M. A. Abushagur, and Z. Lu, *Opt. Express* **16**, 20142 (2008).
- <sup>8</sup>*Plasmonic Nanoguides and Circuits*, edited by S. I. Bozhevolnyi (Pan Stanford, Singapore, 2008).
- <sup>9</sup>A. V. Krasavin and A. V. Zayats, *Phys. Rev. B* **78**, 045425 (2008).
- <sup>10</sup>T. Ogawa, D. F. P. Pile, T. Okamoto, M. Haraguchi, M. Fukui, and D. K. Gramotnev, *J. Appl. Phys.* **104**, 033102 (2008); D. K. Gramotnev and K. C. Vernon, *Appl. Phys. B: Lasers Opt.* **86**, 7 (2007).
- <sup>11</sup>M. Yan and M. Qiu, *J. Opt. Soc. Am. B* **24**, 2333 (2007).
- <sup>12</sup>E. Moreno, S. G. Rodrigo, S. I. Bozhevolnyi, L. Martin-Moreno, and F. J. Garcia-Vidal, *Phys. Rev. Lett.* **100**, 023901 (2008).
- <sup>13</sup>J. Henzie, E.-S. Kwak, and T. W. Odom, *Nano Lett.* **5**, 1199 (2005).
- <sup>14</sup>M. I. Stockman, *Phys. Rev. Lett.* **93**, 137404 (2004).